The Viral State Dynamics of the Discrete-Time NIMFA Epidemic Model

Prasse, Bastian; Van Mieghem, Piet

DOI
10.1109/TNSE.2019.2946592

Publication date
2019

Document Version
Final published version

Published in
IEEE Transactions on Network Science and Engineering

The Viral State Dynamics of the Discrete-Time NIMFA Epidemic Model

Bastian Prasse and Piet Van Mieghem

***Abstract*—The majority of research on epidemics relies on models which are formulated in continuous-time. However, processing real-world epidemic data and simulating epidemics is done digitally and the continuous-time epidemic models are usually approximated by discrete-time models. In general, there is no guarantee that properties of continuous-time epidemic models, such as the stability of equilibria, also hold for the respective discrete-time approximation. We analyse the discrete-time NIMFA epidemic model on directed networks with heterogeneous spreading parameters. In particular, we show that the viral state is increasing and does not overshoot the steady-state, the steady-state is exponentially stable, and we provide linear systems that bound the viral state evolution. Thus, the discrete-time NIMFA model succeeds to capture the qualitative behaviour of a viral spread and provides a powerful means to study real-world epidemics.**

***Index Terms*—Epidemic processes, nonlinear systems.**

I. Introduction

ORIGINATING from the study of infectious human diseases [1], [2], epidemiology has evolved into a field with a broad spectrum of applications, such as the spread of computer viruses, opinions, or social media content [3], [4]. The mutual characteristic of epidemic phenomena is that they can be modelled by a viral infection, i.e. every individual is either infected (with the opinion, social media content, etc.) or healthy. An imperative element for epidemics is the infection of one individual by another, provided that the individuals are linked (for instance by physical proximity). The epidemic model that we consider in this work describes the spread of a virus on a higher level, by merging individuals with similar characteristics (such as residence or age) into groups.

We consider a contact network of N nodes[1]. At any time $t \geq 0$, each node i has a *viral state* $v_i(t)$, which equals to the fraction of infected individuals of group i. If a viral infection is possible from group i to group j, then there is a directed link from node i to node j. For instance, a node could correspond to a geographical region, the viral state $v_i(t)$ could be the ratio of infected individuals in region i and a link could capture a significant flow of people between the respective regions. For node i, the *continuous-time NIMFA model* [5], [6] with heterogeneous spreading parameters describes the viral state evolution by

$$\frac{dv_i(t)}{dt} = -\delta_i v_i(t) + (1 - v_i(t)) \sum_{j=1}^{N} \beta_{ij} v_j(t). \tag{1}$$

Here, $\beta_{ij} \geq 0$ denotes the *infection rate* from group j to group i and $\delta_i > 0$ denotes the *curing rate* of group i. The directed link from node j to node i in the network is weighted by the infection rate β_{ij}. If $\beta_{ij} > 0$, then infections occur from group j to group i. If $\beta_{ii} > 0$, then the members of the same group i infect one another. The *discrete-time NIMFA model* is obtained from the continuous-time NIMFA (1) by applying Euler's method [7], with sampling time $T > 0$, and the discrete-time curing and infection probabilities follow as $q_i = \delta_i T$ and $w_{ij} = \beta_{ij} T$, respectively. For the discretisation, the sampling time T must be "sufficiently small", which we state more precisely in Section IV.

Definition 1 (Discrete-Time NIMFA Model): The discrete-time NIMFA model is given by

$$v_i[k+1] = (1 - q_i) v_i[k] + (1 - v_i[k]) \sum_{j=1}^{N} w_{ij} v_j[k] \tag{2}$$

for every group $i = 1, \ldots, N$, where $k \in \mathbb{N}$ denotes the discrete time slot, $q_i > 0$ is the discrete-time *curing probability*, and $w_{ij} \geq 0$ is the discrete-time *infection probability* from group j to group i.

As vector equations, (2) reads

$$v[k+1] = \operatorname{diag}(u - q) v[k] + \operatorname{diag}(u - v[k]) W v[k], \tag{3}$$

where the viral state vector at discrete time k equals $v[k] = (v_1[k], \ldots, v_N[k])^T$, the curing probability vector equals $q = (q_1, \ldots, q_N)^T$, the $N \times N$ infection probability matrix W is composed of the elements w_{ij}, and u is the $N \times 1$ all-one vector. The *steady-state*[2] *vector* v_∞ of the discrete-time NIMFA model (3) is significant, because it corresponds to the endemic state of the disease in the network.

Definition 2 (Steady-State Vector): The steady-state vector $v_\infty = (v_{\infty,1}, \ldots, v_{\infty,N})^T$ is, if existent, the non-zero equilibrium of the discrete-time NIMFA model (2), which satisfies

Manuscript received March 14, 2019; revised September 27, 2019; accepted October 5, 2019. Date of publication October 10, 2019; date of current version September 2, 2020. Recommended for acceptance by G. Xiao. *(Corresponding author: Bastian Prasse.)*

The authors are with the Departments of Electrical Engineering, Mathematics and Computer Science, Delft University of Technology, 2628 CD Delft, The Netherlands (e-mail: b.prasse@tudelft.nl; p.f.a.vanmieghem@tudelft.nl).

This paper has supplementary downloadable material available at http://ieeexplore.ieee.org, provided by the authors.

Digital Object Identifier 10.1109/TNSE.2019.2946592

[1] In this work, we use the words group and node interchangeably.

[2] Strictly speaking, the origin $v[k] = 0$ is always a steady-state of the NIMFA model (2). With slight abuse of notation, we only refer to the non-zero equilibrium v_∞, but not to the zero equilibrium $v[k] = 0$, as steady-state.

$$\sum_{j=1}^{N} w_{ij} v_{\infty,j} = q_i \frac{v_{\infty,i}}{1 - v_{\infty,i}}, \quad i = 1, \dots, N. \tag{4}$$

We argue that *the discrete-time NIMFA system (3) is (one of) the simplest epidemic models that meets the practical requirements of modelling real-world epidemics on networks.* In particular, the NIMFA system succeeds to exhibit the following six properties, which are crucial for modelling and processing real-world epidemic data:

- P1. Every node i can be interpreted as a *group* of individuals. In theory, modelling an epidemic per individual may be more accurate than combining individuals into groups. However, it is infeasible in practice to determine the viral state of *every individual at every time* t. A more realistic approach is to sample a subset of individuals to obtain an estimate of the viral state of a group. Ideally, the individuals in a same group are exchangeable and indistinguishable.
- P2. The viral state v evolves in discrete time k, which is advantageous for two reasons. First, for the simulation of a viral spread, an implicit discretisation is performed for the majority of continuous-time epidemic models due to the absence of closed-form solutions for the viral state $v(t)$. Hence, a more accurate approach is to directly study the epidemic model in discrete-time. Second, data on real-world epidemics is often collected periodically[3] and discrete-time models circumvent the incomplete knowledge of the viral state of time spans between two measurements.
- P3. Node j infects node i if there is a directed link from node j to node i. More specifically, the NIMFA model (2) accounts for the infection from group j to group i by the term $(w_{ij}(1 - v_i[k])v_j[k])$, which is proportional to both the fraction $(1 - v_i[k])$ of healthy individuals of group i at time k and the fraction $v_j[k]$ of infected individuals of group j at time k. The infection probability w_{ij} measures the contact probability between group i and j (e.g., group i and j could be two geographical regions that are either adjacent or far apart).
- P4. There is a curing term that opposes the infection of node i by its neighbours. In particular, the curing term $(1 - q_i)v_i[k]$ of group i in the NIMFA model (2) is proportional to the fraction $v_i[k]$ of infected individuals of group i. The curing probability q_i measures the capacity of the group i to heal from the virus (which can be heterogeneous since a group may, e.g., refer to either young or old individuals).
- P5. There is a unique [8], [9] non-zero equilibrium v_∞, which corresponds to the endemic state of the virus. Furthermore, if the disease does not die out, then the viral state v approaches the endemic viral state v_∞, i.e. $v[k] \to v_\infty$ for $k \to \infty$, which we show in this work. To the best of our knowledge, the convergence of the viral state $v(t)$ to the steady-state v_∞ has only been shown [5], [10] for the *continuous-time* NIMFA model (1).
- P6. The viral state is increasing, i.e. $v_i[k] > v_i[k-1]$ for any node i at any time k, provided that the disease does not die out and the initial viral state $v[1]$ is close to zero (almost disease-free), which we show in this work. The viral state v_i of node i often refers to *cumulative* variables in practical applications, which are increasing and close to zero at the beginning of the outbreak of the disease. For instance [9], the viral state $v_i[k]$ of node i may refer to the fraction of deaths by cholera of group i up to time k.

For real-world applications, the usefulness of an epidemic model does not reduce to solely satisfying the properties P1–P6. An epidemic model must additionally be capable of giving answers to questions which are relevant to practical use-cases. In particular, we identify three questions.

- Q1. In view of the absence of a closed-form solution of the NIMFA difference equation (2), *is there an approximate and simpler description of the viral state evolution?* Of particular interest is a worst-case scenario of the viral spread, i.e. an upper bound of the viral state $v_i[k]$ for any node i at any time k.
- Q2. *How quickly does the virus spread?* I.e. how fast does the viral state $v[k]$ approach the steady-state v_∞?
- Q3. *How to fit the NIMFA model (2) to real-world data?* In applications, we do not (exactly) know the infection probability matrix W or the curing probabilities q. In recent works [9], [11], efficient methods were derived for learning the spreading parameters W, q of the NIMFA model (2) from viral state $v[k]$ observations. A great advantage for the estimation of the spreading parameters q, W is the linearity of the NIMFA equations (2) with respect to q, W.

In this work, we answer the questions Q1 and Q2. In summary, the NIMFA system (2) is a well-behaved and powerful model, which can be fit to various epidemic data due to the full heterogeneity of the spreading parameters W, q. In Section II, we review related work. The nomenclature and assumptions are introduced in Section III and Section IV, respectively. In Section V, we analyse the viral state dynamics for large times k. We study the monotonicity of the viral state evolution in Section VI. In Section VII, we derive upper and lower bounds on the viral state dynamics.

II. Related Work

On the one hand, in [5], [8], [9], [11], [12], the continuous-time NIMFA model (1), and variants thereof, are considered as the *exact* description of the viral state evolution and every node i corresponds to a group of individuals. We emphasise that the NIMFA equations (1) are a special case of the epidemic model which was originally proposed by Lajmanovich *et al.* [5].

[3] For instance, the German Robert Koch Institute gathers and provides online access to cases of notifiable diseases with the web-based query system *SurvStat@RKI 2.0* on a weekly basis.

TABLE I
NOMENCLATURE

β_{ij}	Continuous-time infection rate from group j to group i
δ_i	Continuous-time curing rate of group i
$\mathrm{diag}(x)$	For a vector $x \in \mathbb{R}^N$, $\mathrm{diag}(x)$ is the $N \times N$ diagonal matrix with x on its diagonal
I	The $N \times N$ identity matrix
$\lambda_1(M)$	Eigenvalue with the largest real part of a square matrix M
N	Number of nodes
q	Discrete-time curing probability vector; $q = (q_1, ..., q_N)^T$ and $q_i = \delta_i T$
$q_{\min}$	Minimal discrete-time curing probability; $q_{\min} = \min\{q_1, ..., q_N\}$
R	$N \times N$ matrix $R = I - \mathrm{diag}(q) + W$
$\rho(M)$	Spectral radius of a square matrix M
T	Sampling time of the discrete-time NIMFA model
u	All-one vector $u = (1, ..., 1)^T \in \mathbb{R}^N$
$v[k]$	Viral state $v[k] = (v_1[k], ..., v_N[k])^T$ at discrete time $k \in \mathbb{N}$; $v_i[k] \in [0, 1]$ for $i = 1, ..., N$
v_∞	Steady state vector, the non-zero equilibrium of (2)
$\Delta v[k]$	Difference of the viral state to the steady state; $\Delta v[k] = v[k] - v_\infty$
W	Discrete-time $N \times N$ infection probability matrix; $w_{ij} = \beta_{ij} T$
x_1	Principal eigenvector of the matrix R; $Rx_1 = \rho(R)x_1$

On the other hand, in [6], [13], [14], the NIMFA model was derived as an *approximation* of the susceptible-infected-susceptible (SIS) epidemic process [3], [4] and "NIMFA" is an acronym for "N-Intertwined Mean-Field Approximation". For the SIS process, every node i is usually interpreted as a single individual.

The discrete-time NIMFA model with homogeneous spreading parameters has been studied in [9], [11], [15]. The discrete-time NIMFA model (2) with fully heterogeneous spreading parameters has been proposed by Paré *et al.* [9], who showed that there is either one stable equilibrium, the healthy state $v[k] = 0$, or there are two equilibria, the healthy state and a steady-state v_∞ with positive components. Furthermore, the discrete-time NIMFA model (3) has been validated on data of real-world epidemics [9]. We are not aware of results that assess the stability of the steady-state v_∞ of the discrete-time NIMFA system (2). On the contrary, Ahn *et al.* [15] gave a counterexample for which the steady-state v_∞ of the NIMFA model (3) is unstable. In this work, we extend the analysis of Paré *et al.* [9] and we show that the steady-state v_∞ is exponentially stable, provided that the Assumptions in Section IV hold true.

III. NOMENCLATURE

For a square matrix M, we denote the spectral radius by $\rho(M)$ and the eigenvalue with the largest real part by $\lambda_1(M)$. For two $N \times 1$ vectors y, z, it holds $y > z$ or $y \geq z$ if $y_i > z_i$ or $y_i \geq z_i$, respectively, for every element $i = 1, \ldots, N$. The minimum of the discrete-time curing probabilities is denoted by $q_{\min} = \min\{q_1, \ldots, q_N\}$. We define the $N \times N$ matrix R as

$$R = I - \mathrm{diag}(q) + W. \tag{5}$$

The principal eigenvector of the matrix R is denoted by x_1. Table I summarises the nomenclature.

IV. ASSUMPTIONS

Assumption 1: The curing probabilities are positive and the infection probabilities non-negative, i.e. $q_i > 0$ and $w_{ij} \geq 0$ for all nodes i, j.

Assumption 2: For every node $i = 1, \ldots, N$, the sampling time $T > 0$ satisfies

$$T \leq T_{\max} = \frac{1}{\delta_i + \sum_{j=1}^{N} \beta_{ij}}. \tag{6}$$

The results of this work which rely on Assumption 2 hold true if the sampling time is sufficiently small, which we consider a rather technical assumption. The particular choice of the bound (6) is due to Lemma 3 in Section V. Furthermore, we make the following assumption on the initial viral state $v_i[1]$.

Assumption 3: For every node $i = 1, \ldots, N$, it holds that $0 \leq v_i[1] \leq v_{\infty,i}$.

Assumption 3 is reasonable since the initial viral state $v[1]$ of many real-world epidemics is almost disease-free. For instance, at the beginning of the periodic outbreak of the flu, every geographical region is almost healthy. As another example, consider the spread of content (e.g., a novel tweet or a post) on online social media. The beginning of the epidemic outbreak (at time $k = 1$) would correspond to the first appearance of the online content. Hence, the viral state $v_i[1]$, where node i refers to a group of users, is close to 0.

Assumption 4: The infection probability matrix W is irreducible.

Assumption 4 holds if and only if the infection probability matrix W corresponds to a strongly connected graph[4]. Finally, as shown in [9], Assumption 5 avoids the trivial viral dynamics in which the virus dies out.

[4] In a strongly connected graph, there is a path from every node i to any other node j.

Assumption 5: The spectral radius of the matrix R is greater than one, i.e. $\rho(R) > 1$.

V. Viral State Dynamics Close to the Steady-State

For completeness, we recapitulate the results of Paré *et al.* [9] on the equilibria and the stability of the healthy state[5].

Theorem 1 ([9]): Under Assumptions 1, 2 and 4, the following two statements hold true:

(1) If $\rho(R) \leq 1$, then the healthy state $v[k] = 0$ is the only equilibrium of the discrete-time NIMFA model (3). Furthermore, $v[k] \to 0$ when $k \to \infty$ for any initial viral state $v[1]$ with $0 \leq v_i[1] \leq 1$ for every node i.

(2) If $\rho(R) > 1$, then there are two equilibria of the discrete-time NIMFA model (3): The healthy state $v[k] = 0$ and a steady-state v_∞ with $v_{\infty,i} > 0$ for every node i.

The *basic reproduction number* R_0 of the NIMFA epidemic model [16] equals the spectral radius $\rho(R)$. The NIMFA model with *homogeneous* spreading parameters [6], [17] assumes that there is a scalar curing rate δ and a scalar infection rate β such that $q_i = \delta$ and $\beta_{ij} = \beta a_{ij}$ for all nodes i, j, where a_{ij} denote the elements of a symmetric and irreducible zero-one adjacency matrix A. For the NIMFA model with homogeneous spreading parameters, the condition $\rho(R) \leq 1$ simplifies to $\tau \leq \tau_c^{(1)}$ with the *effective infection rate* $\tau = \beta/\delta$ and the *epidemic threshold* $\tau_c^{(1)} = 1/\lambda_1(A)$.

Lemma 1: Suppose that Assumptions 1, 2 and 4 hold. Then, the matrix R is irreducible and non-negative.

Proof: Appendix A. ∎

Hence, it follows from the Perron-Frobenius Theorem [18] that, under Assumptions 1, 2 and 4, there is a real eigenvalue $\lambda_1(R)$ of the matrix R which equals the spectral radius $\rho(R)$ and that the principal eigenvector x_1 is positive.

We can generalise the bounds from [6], [13] for the steady-state vector v_∞ to the NIMFA model (2) with heterogeneous spreading parameters.

Lemma 2: Suppose that Assumptions 1, 2, 4 and 5 hold. Then, the steady-state $v_{\infty,i}$ of any node i is bounded by

$$1 - \frac{q_i}{\sum_{j=1}^N w_{ij}} \leq v_{\infty,i} \leq 1 - \frac{q_i}{q_i + \sum_{j=1}^N w_{ij}}.$$

Proof: Appendix B. ∎

We denote the difference of the viral state $v[k]$ to the steady state v_∞ by $\Delta v[k] = v[k] - v_\infty$. By considering the difference $\Delta v[k] = v[k] - v_\infty$, we obtain an equivalent representation[6] of the discrete-time NIMFA equations (2).

Proposition 1 (NIMFA Equations as Difference to the Steady-State): Suppose that Assumptions 1, 2, 4 and 5 hold. Then, the difference $\Delta v[k] = v[k] - v_\infty$ from the viral state $v[k]$ to the steady state v_∞ of the discrete-time NIMFA model (3) evolves according to

$$\Delta v[k+1] = F\Delta v[k] - \operatorname{diag}(\Delta v[k]) W \Delta v[k], \tag{7}$$

where the $N \times N$ matrix F is given by

$$F = I + \operatorname{diag}\left(\frac{q_1}{v_{\infty,1} - 1}, \ldots, \frac{q_N}{v_{\infty,N} - 1}\right) + \operatorname{diag}(u - v_\infty) W. \tag{8}$$

Proof: Appendix C. ∎

For a sufficiently small sampling time T, Lemma 3 states that every element of matrix F is non-negative.

Lemma 3: Suppose that Assumptions 1, 2, 4 and 5 hold. Then, the $N \times N$ matrix F defined by (8) is non-negative, i.e. $(F)_{ij} \geq 0$ for every $i, j = 1, \ldots, N$.

Proof: Appendix D. ∎

Furthermore, Proposition 1 leads to the following corollary.[7]

Corollary 1: Suppose that Assumption 1–5 hold. Then, it holds that $v_i[k] \leq v_{\infty,i}$ for every node i at every time $k \geq 1$.

Proof: Appendix E. ∎

In other words, Corollary 1 states that the set $\mathcal{V} = \{v | 0 \leq v_i \leq v_{\infty,i},\ \forall i = 1, \ldots, N\}$ is a *positive invariant set* [19] of the NIMFA model (2), i.e., if the initial viral state $v[1]$ is element of the set $\mathcal{V}$, then the viral state $v[k]$ will remain in the set $\mathcal{V}$ for $k \geq 1$. We emphasise that Corollary 1 does not imply that the viral state $v[k]$ increases monotonically.

To provide a graphical illustration of Corollary 1, we generate a random network with $N = 10$ nodes by creating a directed link $a_{ij} = 1$ from any node j to any node i with probability 0.25 and we repeat this network generation if the resulting network is not strongly connected. If $a_{ij} = 1$, then we set the infection probability w_{ij} to a uniformly distributed random number in [0, 1] and, if $a_{ij} = 0$, then we set $w_{ij} = 0$. The curing probability q_i for every node i is set to a uniformly distributed random number in $[0.95c, 1.05c]$, where $c = 10$ is a constant. If the spectral radius $\rho(R) \leq 1 + 10^{-3}$, then we set the constant c to $c/1.1$ and generate new curing probabilities q and we repeat this generation of curing probabilities q until $\rho(R) > 1 + 10^{-3}$. The sampling time T is set to $T = T_{\max}/10$, given by (6). For every node i, the initial viral state $v_i[1]$ is set to a uniformly distributed random number in $[0, 0.01v_{\infty,i}]$. Fig. 1 depicts the resulting viral state traces $v_i[k]$ for every node i. As stated by Corollary 1, the viral state $v[k]$ approaches the steady state v_∞ from below without overshooting, but the viral state $v[k]$ is not strictly increasing. The absence of overshoot is not evident, e.g., in a Markovian SIS process overshoot is possible [20].

For applications in which the initial viral state $v[1]$ is close to zero, the NIMFA equations (9) can be replaced by linear time-invariant (LTI) systems in two different regimes: On the one hand, it holds for small times k that $v[k] \approx 0$. Hence, the representation (3) can be linearised around the origin $v[k] = 0$, which yields

$$v[k+1] \approx Rv[k], \tag{9}$$

[5] Theorem 1 follows immediately from merging [9, Theorems 1-2 and Proposition 2].

[6] Proposition 1 is a generalisation of [11, Proposition 3] to the NIMFA model with heterogeneous spreading parameters q, W.

[7] Corollary 1 is a generalisation of [11, Corollary 1] to the NIMFA model with heterogeneous spreading parameters q, W.

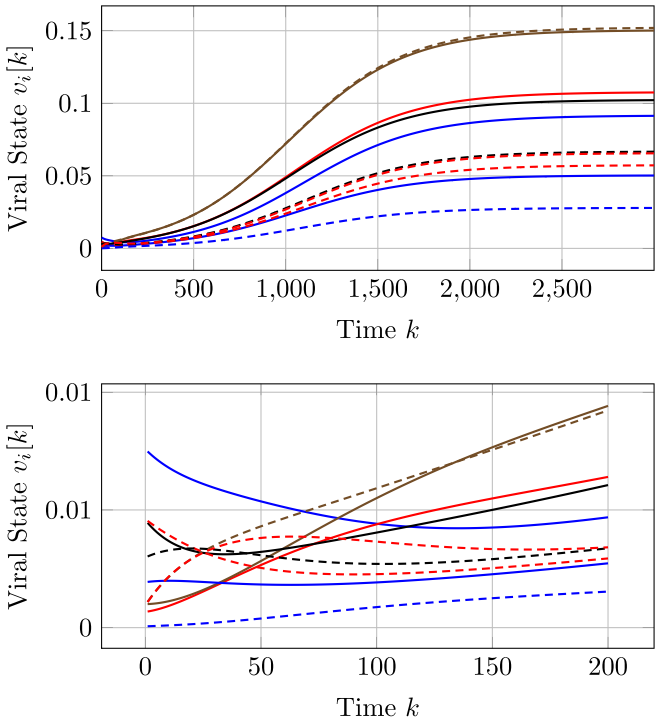

Fig. 1. The upper sub-plot depicts the viral state traces $v_i[k], i = 1, \ldots, N$, for a directed network with $N = 10$ nodes and heterogeneous spreading parameters q, W until discrete time $k = 3000$. The lower sub-plot depicts the same viral state traces $v_i[k], i = 1, \ldots, N$, but only the initial phase until discrete time $k = 200$.

for small times k. On the other hand, if the viral state $v[k]$ is close to the steady-state v_∞, which implies $\Delta v[k] \approx 0$, then the representation (7) can be linearised around the origin $\Delta v[k] = 0$, which gives

$$\Delta v[k+1] \approx F \Delta v[k]. \tag{10}$$

Furthermore, we obtain that the steady-state v_∞ is asymptotically stable[8].

Theorem 2 (Asymptotic Stability of the Steady-State): Under Assumptions 1, 2, 4 and 5, the steady-state v_∞ of the discrete-time NIMFA system (3) is asymptotically stable.

Proof: Appendix F. ■

Ahn *et al.* [15] gave a counterexample for which the steady-state v_∞ of the discrete-time NIMFA system (3) is unstable. However, their counterexample does not satisfy Assumption 2. Hence, a sufficiently small sampling time T is decisive for the stability of the discrete-time NIMFA model (3). (Paré *et al.* [9] observed that the counterexample in [15] violates the third assumption in [9], which is closely related to Assumption 2.)

VI. Monotonicity of the Viral State Dynamics

As stated by the property P6 in Section I, we will show that the viral state $v[k]$ is increasing, provided that the initial viral state $v[1]$ is small.

Definition 3 (Strictly Increasing Viral State Evolution): The viral state $v[k]$ is *strictly increasing at time* k if $v[k+1] > v[k]$. The viral state $v[k]$ is *globally strictly increasing* if $v[k]$ is strictly increasing at every time $k \geq 1$.

Lemma 4 states an inductive property of the monotonicity.

Lemma 4: Under Assumptions 1–5, the viral state $v[k]$ is strictly increasing at time k if the viral state $v[k-1]$ is strictly increasing at time $k-1$.

Proof: Appendix G. ■

For any vector $y = (y_1, \ldots, y_N)^T$ we define $y^l = (y_1^l, \ldots, y_N^l)^T$. Theorem 3 states equivalent conditions to a globally strictly increasing viral state evolution.

Theorem 3 (Monotonicity of the Viral State Evolution): Suppose that Assumptions 1–5 hold. Then, the viral state $v[k]$ is globally strictly increasing if and only if one of the following two (equivalent) statements holds:

(1) The initial viral state $v[1]$ satisfies

$$(W - \operatorname{diag}(q))v[1] > \operatorname{diag}(q) \sum_{l=2}^{\infty} v^l[1]. \tag{11}$$

(2) It holds

$$(\operatorname{diag}(u - v_\infty) W \operatorname{diag}(u - v_\infty) - \operatorname{diag}(q))z > \operatorname{diag}(q) \sum_{l=2}^{\infty} z^l,$$

where the $N \times 1$ vector z is given by

$$z_i = \frac{v_i[1] - v_{\infty,i}}{1 - v_{\infty,i}}, \quad i = 1, \ldots, N.$$

Proof: Appendix H. ■

For any scalar y with $|y| < 1$, the geometric series $\sum_{l=2}^{\infty} y^l = \frac{y^2}{1-y}$ gives an alternative form of the right-hand sides of statement 1 and 2 of Theorem 3. From Theorem 3, we obtain a corollary which states sufficient conditions for a globally strictly increasing viral state.

Corollary 2: Suppose Assumptions 1–5 hold and that the initial viral state $v[1]$ equals either

$$v[1] = \epsilon x_1 + \eta \tag{12}$$

or

$$v[1] = (1 - \epsilon) v_\infty + \eta$$

for some small $\epsilon > 0$ and an $N \times 1$ vector η whose norm $\|\eta\|_2 = \mathcal{O}(\epsilon^p)$ for some scalar $p > 1$ which is independent of ϵ. Then, there exists an $\epsilon > 0$ such that the viral state $v[k]$ is globally strictly increasing.

Proof: Appendix I. ■

Numerical simulations show that if the initial viral state $v[1]$ approaches zero from an *arbitrary* direction, which differs from (12), then the viral state $v[k]$ is in general *not* globally strictly increasing. However, the simulations also indicate that, if the initial viral state $v[1]$ is small, then the viral state seems "almost" globally strictly increasing, which is illustrated by Fig. 1 and motivates us to state Definition 4.

[8] The steady-state v_∞ is asymptotically stable if there exists an $\epsilon > 0$ such that $\|v[1] - v_\infty\| < \epsilon$ implies that $v[k] \to v_\infty$ when $k \to \infty$.

Definition 4 (Quasi-Increasing Viral State Evolution): Define S_- as the set of times $k \geq 1$ at which the viral state $v[k]$ is not strictly increasing:

$$S_- = \{k \in \mathbb{N} \mid \exists i : \ v_i[k+1] \leq v_i[k]\}.$$

Then, the viral state $v[k]$ is *quasi-increasing with stringency* ϵ, if the set S_- is finite and $\|v[k+1] - v[k]\|_2 \leq \epsilon$ for every time k in S_-.

Thus, a quasi-increasing viral state $v[k]$ is strictly increasing at every time k not in the set S_- and at the times k in the finite set S_-, the viral state $v[k]$ is decreasing only within an ϵ-stringency. For the viral state trace $v[k]$ depicted in Fig. 1, the set S_- equals $S_- = \{1, 2, \ldots, 165\}$. Theorem 4 states that the viral state $v[k]$ is quasi-increasing with an arbitrarily small stringency ϵ, provided that the initial viral state $v[1]$ is sufficiently small.

Theorem 4: Suppose that Assumptions 1–5 hold and that $v[1] \neq 0$. Then, for any $\epsilon > 0$ there is a $\vartheta(\epsilon)$ such that $\|v[1]\|_2 \leq \vartheta(\epsilon)$ implies that the viral state $v[k]$ is quasi-increasing with stringency ϵ.

Proof: Appendix J. ■

VII. Bounds on the Viral State Dynamics

Due to the non-linearity of the NIMFA equations (3), an analysis of the *exact* viral state evolution is challenging. However, it is possible to upper- and lower-bound the viral state $v[k]$ by LTI systems, which allows for an *approximate* analysis of the viral state evolution. As stated by Proposition 2, the linearisation (9) of the NIMFA model around zero directly yields an upper bound on the viral state $v[k]$.

Proposition 2 (First Upper Bound): Suppose that Assumptions 1–3 hold and define the LTI system

$$v_{\mathrm{ub}}^{(1)}[k+1] = R v_{\mathrm{ub}}^{(1)}[k], \quad k \geq 1, \tag{13}$$

where the matrix R is given by (5). If $v_{\mathrm{ub}}^{(1)}[1] \geq v[1]$, then it holds that $v_{\mathrm{ub}}^{(1)}[k] \geq v[k]$ at every time $k \geq 1$. If $\rho(R) \geq 1$, then the LTI system (13) is unstable. If $\rho(R) < 1$, then the LTI system (13) is asymptotically stable.

Proof: Appendix K. ■

In addition the upper bound in Proposition 2, the linearisation (10) of the NIMFA model around the steady-state v_∞ yields another upper bound on the viral state $v[k]$, as stated by Proposition 3.

Proposition 3 (Second Upper Bound): Under Assumptions 1–5, denote an upper bound of the difference of the viral state $v[k]$ to the steady-state v_∞ at time k by $\Delta v_{\mathrm{ub}}[k]$. Furthermore, define the LTI system

$$\Delta v_{\mathrm{ub}}[k+1] = F \Delta v_{\mathrm{ub}}[k], \quad k \geq 1, \tag{14}$$

where the $N \times N$ matrix F is given by (8). Then, the following statements hold true:

(1) If $\Delta v_{\mathrm{ub}}[1] \geq \Delta v[1]$, then it holds that $\Delta v_{\mathrm{ub}}[k] \geq \Delta v[k]$ at every time $k \geq 1$.
(2) If $\Delta v_{\mathrm{ub}}[1] \leq 0$, then it holds that $\Delta v_{\mathrm{ub}}[k] \leq 0$ at every time k.

Proof: Appendix L. ■

Hence, the LTI system (14) yields the upper bound

$$v_{\mathrm{ub}}^{(2)}[k] := \Delta v_{\mathrm{ub}}[k] + v_\infty \geq v[k]$$

on the viral state $v[k]$ at every time k. If Assumption 3 holds and $\Delta v_{\mathrm{ub}}[1] = \Delta v[1]$, then it holds that $0 \geq \Delta v_{\mathrm{ub}}[k] \geq \Delta v[k]$ for every time k. Thus, the convergence of $\Delta v[k]$ to 0 implies the convergence of $\Delta v_{\mathrm{ub}}[k]$ to 0. The upper bound of Proposition 2 is tight when the viral state $v[k]$ is small and the upper bound of Proposition 3 is tight when the viral state $v[k]$ is close to the steady-state v_∞. We combine Propositions 2 and 3 to obtain a tighter upper bound, for every node $i = 1, \ldots, N$, as

$$v_{\mathrm{ub},i}[k] := \min\{v_{\mathrm{ub},i}^{(1)}[k], v_{\mathrm{ub},i}^{(2)}[k]\}. \tag{15}$$

Finally, Proposition 4 provides a lower bound on the viral state $v[k]$.

Proposition 4 (Lower Bound): Suppose that Assumptions 1–5 hold and let there be an $N \times 1$ vector $v_{\min} > 0$ such that $v[k] \geq v_{\min}$ holds at every time $k \geq 1$. Furthermore, let $\Delta v_{\mathrm{lb}}[1] = \Delta v[1]$ and define the LTI system

$$\Delta v_{\mathrm{lb}}[k+1] = F_{\mathrm{lb}} \Delta v_{\mathrm{lb}}[k], \quad k \geq 1, \tag{16}$$

where the $N \times N$ matrix F_{lb} is given by

$$F_{\mathrm{lb}} = I + \mathrm{diag}\left(\frac{q_1}{v_{\infty,1} - 1}, \ldots, \frac{q_N}{v_{\infty,N} - 1}\right) + \mathrm{diag}(u - v_{\min})W.$$

Then, the following statements hold true:

(1) It holds that $\Delta v_{\mathrm{lb}}[k] \leq \Delta v[k] \leq 0$ at every time $k \geq 1$.
(2) Denote $\gamma = \min\{v_{\min,1}, \ldots, v_{\min,N}\}$. Then, it holds

$$\Delta v_{\mathrm{lb}}[k] \geq -\left(1 - q_{\min}\frac{\gamma}{1-\gamma}\right)^{k-1} v_\infty.$$

Hence, $\Delta v_{\mathrm{lb}}[k] \to 0$ when $k \to \infty$.

Proof: Appendix M. ■

Hence, the LTI system (16) yields the lower bound

$$v_{\mathrm{lb}}[k] := \Delta v_{\mathrm{lb}}[k] + v_\infty \leq v[k] \tag{17}$$

on the viral state $v[k]$ at every time k. In particular, if the viral state $v[k]$ is globally strictly increasing, as discussed in Section VI, then the vector $v_{\min}$ can be chosen as $v_{\min} = v[1]$. Lemma 5 ensures the existence of a vector $v_{\min} > 0$ for every initial viral state $v[1] \neq 0$, which can be applied to Proposition 4.

Lemma 5: Suppose that Assumptions 1–5 hold. Then, for any initial viral state $v[1] > 0$, there exists an $N \times 1$ vector $v_{\min} > 0$ such that $v[k] \geq v_{\min}$ holds at every time $k \geq 1$. Furthermore, for any initial viral state $v[1] \neq 0$, there exists an $N \times 1$ vector $v_{\min} > 0$ such that $v[k] \geq v_{\min}$ holds at every time $k \geq N - 1$.

Proof: Appendix N. ■

Proposition 4 and Lemma 5 guarantee the existence of an LTI system (16) that lower-bounds the viral state $v[k]$. Thus,

the viral state $v[k]$ converges to the steady-state v_∞ exponentially fast:

Corollary 3 (Steady-State is Exponentially Stable): Suppose that Assumptions 1–5 hold. Then, for any initial viral state $v[1] \neq 0$ there exist constants $\alpha < 1$ and $k^* \leq N-1$ such that

$$\|v[k] - v_\infty\|_2 \leq \|v_\infty\|_2 \alpha^{k-1} \quad \forall k \geq k^*. \tag{18}$$

If the initial viral state $v[1] > 0$, then the constant k^* can be set to $k^* = 1$. Furthermore, if the viral state $v[k]$ is globally strictly increasing (cf. Theorem 3) and $v[1] > 0$, then (18) is satisfied for

$$\alpha = 1 - q_{\min} \frac{\gamma}{1-\gamma}, \tag{19}$$

where $\gamma = \min\{v_1[1], \ldots, v_N[1]\}$.

Proof: Appendix O. ∎

It is an open problem whether the steady-state v_∞ is exponentially stable for initial viral states $v[1]$ that do not satisfy Assumption 3. In the susceptible-infected-susceptible (SIS) epidemic process [3], [21], the *hitting time* T_{H_n} is the first time when the SIS process reaches a state with n infected nodes. As argued in [22], the average hitting time $\mathrm{E}[T_{H_n}]$ scales exponentially with respect to the number n of infected nodes, which is in agreement with the exponential convergence to the steady state v_∞ for the NIMFA epidemic model.[9]

We provide a numerical evaluation of the upper bound $v_{\mathrm{ub}}[k]$, given by (15), and the lower bound $v_{\mathrm{lb}}[k]$, given by (17). We generate a directed Erdős-Rényi random graph with $N = 500$ nodes by creating a directed link $a_{ij} = 1$ from any node j to any node i with link probability 0.05. We generate another graph if the resulting graph is not strongly connected. If $a_{ij} = 1$, then we set the infection probability w_{ij} to a uniformly distributed random number in [0, 1] and, if $a_{ij} = 0$, then we set $w_{ij} = 0$. The curing probability q_i for every node i is set to a uniformly distributed random number in $[0.95c, 1.05c]$, where $c = 10$ is a constant. If the spectral radius $\rho(R) \leq 1 + 10^{-5}$, then we set the constant c to $c/1.005$ and generate new curing probabilities q and we repeat this generation of curing probabilities q until $\rho(R) > 1 + 10^{-5}$. The sampling time T is set to $T = T_{\max}/20$, given by (6). For every node i, the initial viral state $v_i[1]$ is set to a uniformly distributed random number $[0, 0.1v_{\infty,i}]$. We initialise the bounds $v_{\mathrm{ub}}[k]$ and $v_{\mathrm{lb}}[k]$ on the viral state $v[k]$ at different bound-initialisation times $k_0 \geq 1$, i.e., $v_{\mathrm{lb}}[k_0] = v[k_0] = v_{\mathrm{ub}}[k_0]$. To obtain the lower bound $v_{\mathrm{lb}}[k]$, we set the vector $v_{\min}$ of Proposition 4 to

$$v_{\min,i} = \min_{k \geq k_0} v_i[k], \quad i = 1, \ldots, N.$$

[9] For an SIS process, the *spreading time* [23] is another measure for the time of convergence to the metastable state. For the spreading time, the convergence to the metastable state is defined differently for every realisation of the same SIS epidemic process. Hence, the spreading time is subject to random fluctuations, which approximately follow a lognormal distribution [22], contrary to the deterministic NIMFA model (2) and the average hitting time $\mathrm{E}[T_{H_n}]$ of an SIS process.

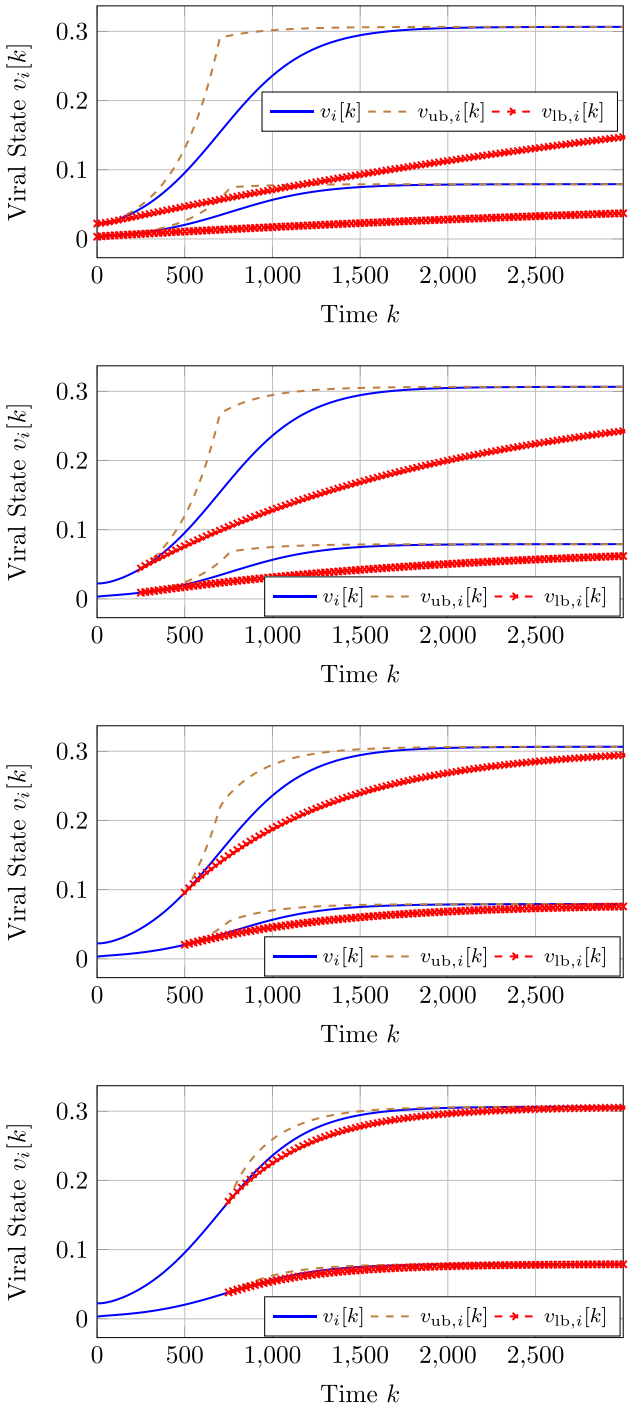

Fig. 2. For a directed Erdős-Rényi random graph with $N = 500$ nodes and heterogeneous spreading parameters q, W, the fit of the lower bound $v_{\mathrm{lb}}[k]$ and the upper bound $v_{\mathrm{ub}}[k]$ on the viral state $v[k]$ is depicted. Each of the four sub-plots shows two viral state traces $v_i[k]$ and the corresponding bounds of the two nodes with the maximal and minimal steady-state $v_{\infty,i}$, respectively. From top to bottom, the sub-plots correspond to an initialisation of the bounds $v_{\mathrm{lb}}[k_0] = v[k_0] = v_{\mathrm{ub}}[k_0]$ at the bound-initialisation time $k_0 = 1$, $k_0 = 250$, $k_0 = 500$ and $k_0 = 750$, respectively.

We emphasise that if $v_i[k_0] > v_i[k_0 - 1]$ holds for every node i, then the vector $v_{\min}$ becomes $v_{\min} = v[k_0]$ due to Lemma 4. Fig. 2 illustrates that, for a small bound-initialisation time k_0, the upper bound $v_{\mathrm{ub}}[k]$ results in a reasonable fit, whereas the lower bound $v_{\mathrm{lb}}[k]$ does not perform well. If the

bound-initialisation time k_0 is greater, then both bounds $v_{\mathrm{lb}}[k]$ and $v_{\mathrm{ub}}[k]$ give a tight fit to the exact viral state $v[k]$.

VIII. Conclusion

In this work, we analysed the discrete-time NIMFA epidemic model with heterogeneous spreading parameters on directed graphs. Our contribution is threefold. First, we proved that the steady-state v_∞ is asymptotically stable and we showed that the viral state $v[k]$ approaches the steady-state v_∞ without overshooting. Second, provided that the initial viral state $v[1]$ is sufficiently small, we showed that the viral state $v[k]$ is increasing. Third, we derived linear systems that give upper and lower bounds on the viral state $v[k]$ and we proved that the viral state $v[k]$ converges to the steady-state v_∞ exponentially fast.

The properties listed as the first and second contribution are phenomena that occur in many real-world epidemics, in particular when the viral state $v[k]$ refers to a cumulative variable (for instance, a fraction of individuals that have shared particular online social media content up to time k).

In conclusion, we have shown that the discrete-time NIMFA epidemic model captures the *qualitative* behaviour of real-world epidemics in which the virus reaches an endemic state. Furthermore, since the spreading parameters are heterogeneous and the underlying contact network is directed, the NIMFA model has a vast parameter space and can be fitted to various real-world epidemic data, which allows for *quantitative* predictions of the viral state evolution.

Acknowledgement

The authors would like to thank Q. Liu for helpful discussions on this material.

References

[1] N. T. J. Bailey, *The Mathematical Theory of Infectious Diseases and Its Applications*, 2nd ed. London, U.K.: Griffin, 1975.
[2] R. M. Anderson and R. M. May, *Infectious Diseases of Humans: Dynamics and Control*. London, U.K.: Oxford Univ. Press, 1992.
[3] R. Pastor-Satorras, C. Castellano, P. Van Mieghem, and A. Vespignani, "Epidemic processes in complex networks," *Rev.Modern Phys.*, vol. 87, no. 3, 2015, Art. no. p. 925.
[4] C. Nowzari, V. M. Preciado, and G. J. Pappas, "Analysis and control of epidemics: A survey of spreading processes on complex networks," *IEEE Control Syst. Mag.*, vol. 36, no. 1, pp. 26–46, Feb. 2016.
[5] A. Lajmanovich and J. A. Yorke, "A deterministic model for gonorrhea in a nonhomogeneous population," *Math. Biosci.*, vol. 28, no. 3–4, pp. 221–236, 1976.
[6] P. Van Mieghem, J. Omic, and R. Kooij, "Virus spread in networks," *IEEE/ACM Trans. Netw.*, vol. 17, no. 1, pp. 1–14, Feb. 2009.
[7] J. Stoer and R. Bulirsch, *Introduction to Numerical Analysis*. Berlin, Germany: Springer, 2013, vol. 12.
[8] A. Fall, A. Iggidr, G. Sallet, and J.-J. Tewa, "Epidemiological models and Lyapunov functions," *Math. Model. Natural Phenomena*, vol. 2, no. 1, pp. 62–83, 2007.
[9] P. E. Paré, J. Liu, C. L. Beck, B. E. Kirwan, and T. Başar, "Analysis, estimation, and validation of discrete-time epidemic processes," *IEEE Trans. Control Syst. Technol.*, 10, Oct. 2018.
[10] A. Khanafer, T. Başar, and B. Gharesifard, "Stability of epidemic models over directed graphs: A positive systems approach," *Automatica*, vol. 74, pp. 126–134, 2016.
[11] B. Prasse and P. Van Mieghem, "Network reconstruction and prediction of epidemic outbreaks for NIMFA processes," *arXiv:1811.06741*, 16, Nov. 2018.
[12] Y. Wan, S. Roy, and A. Saberi, "Designing spatially heterogeneous strategies for control of virus spread," *IET Syst. Biol.*, vol. 2, no. 4, pp. 184–201, 2008.
[13] P. Van Mieghem and J. Omic, "In-homogeneous virus spread in networks," *arXiv:1306.2588*, 2014.
[14] K. Devriendt and P. Van Mieghem, "Unified mean-field framework for susceptible-infected-susceptible epidemics on networks, based on graph partitioning and the isoperimetric inequality," *Phys. Rev. E*, vol. 96, no. 5, 2017, Art. no. 052314.
[15] H. J. Ahn and B. Hassibi, "Global dynamics of epidemic spread over complex networks," in *Proc. 52nd IEEE Conf. Decis. Control*, 2013, pp. 4579–4585.
[16] O. Diekmann, H. Heesterbeek, and T. Britton, *Mathematical Tools for Understanding Infectious Disease Dynamics*. Princeton, NJ, USA: Princeton Univ. Press, 2012.
[17] P. Van Mieghem, "The N-Intertwined SIS epidemic network model," *Computing*, vol. 93, no. 2–4, pp. 147–169, 2011.
[18] P. Van Mieghem, *Graph Spectra for Complex Networks*. New York, NY, USA: Cambridge Univ. Press, 2010.
[19] H. K. Khalil, *Nonlinear Systems*. New Jersey, USA: Prentice-Hall, vol. 2, no. 5, pp. 5–1, 1996.
[20] P. Van Mieghem, "Universality of the SIS prevalence in networks," *arXiv:1612.01386*, 5, Dec. 2016.
[21] D. J. Daley and J. Gani, *Epidemic Modelling: An Introduction*. New York, NY, USA: Cambridge Univ. Press, 2001, vol. 15.
[22] Z. He and P. Van Mieghem, "The spreading time in SIS epidemics on networks," *Phys. A: Statist. Mech. Appl.*, vol. 494, pp. 317–330, 2018.
[23] R. Van de Bovenkamp and P. Van Mieghem, "Time to metastable state in SIS epidemics on graphs," in *Proc. 10th Int. Conf. Signal-Image Technol. Internet-Based Syst.*, 2014, pp. 347–354.
[24] R. A. Horn and C. R. Johnson, *Matrix Analysis*. New York, NY, USA: Cambridge Univ. Press, 1990.

Bastian Prasse received the B.Sc. degree in computer engineering (*Dean's List*) from RWTH Aachen University, Aachen, Germany, in 2012, the M.Sc. degree in systems and control theory from the Royal Institute of Technology (KTH), Stockholm, Sweden, and the M.Sc. degree in computer engineering (*Dean's List*) at RWTH Aachen University, Aachen, Germany, both in 2015. Since April 2017, he has been working toward the Ph.D. degree at Delft University of Technology, Delft, The Netherlands. His main research interests include network reconstruction, systems theory, and optimisation.

Piet Van Mieghem received the master's (*magna cum laude*) and Ph.D. (*summa cum laude*) degrees in electrical engineering from the K.U. Leuven, Leuven, Belgium, in 1987 and 1991.

Since 1998, he is a Professor with the Delft University of Technology and Chairman of the section Network Architectures and Services (NAS). Before joining Delft, he worked at the Interuniversity Micro Electronic Center (IMEC) from 1987 to 1991. During 1993–1998, he was a member of the Alcatel Corporate Research Center in Antwerp, Belgium. He was a Visiting Scientist with MIT (1992–1993), a Visiting Professor with UCLA (2005), a Visiting Professor with Cornell University (2009), and at Stanford University (2015). His main research interests lie in modeling and analysis of complex networks and in new Internet-like architectures and algorithms for future communications networks. He is the author of four books: *Performance Analysis of Communications Networks and Systems* (Cambridge Univ. Press, 2006), *Data Communications Networking* (Techne, 2011), *Graph Spectra for Complex Networks* (Cambridge Univ. Press, 2011), and *Performance Analysis of Complex Networks and Systems* (Cambridge Univ. Press, 2014). He was member of the editorial board of Computer Networks (2005–2006), the IEEE/ACM Transactions on Networking (2008–2012), the *Journal of Discrete Mathematics* (2012–2014) and *Computer Communications* (2012–2015). He is currently on the editorial board of the *OUP Journal of Complex Networks*.